scientific reports

OPEN

Synergistic anti-cancer effect of sodium pentaborate pentahydrate, curcumin and piperine on hepatocellular carcinoma cells

Zehra Omeroglu Ulu[1], Nurdan Sena Degirmenci[1,2], Zeynep Busra Bolat[1,3,4,5] & Fikrettin Sahin[1✉]

Hepatocellular carcinoma (HCC) is a leading cause of cancer-related death in the world. Poor prognosis of HCC patients is a major issue, thus, better treatment options for patients are required. Curcumin (Cur), hydrophobic polyphenol of the plant turmeric, shows anti-proliferative, apoptotic, and anti-oxidative properties. Boron is a trace element which is essential part of human nutrition. Sodium pentaborate pentahydrate (NaB), a boron derivative, is an effective agent against cancer. In the current study, we performed in vitro experiments and transcriptome analysis to determine the response of NaB, Cur, piperine (Pip) and their combination in two different HCC cell lines, HepG2 and Hep3B. NaB and Cur induced cytotoxicity in a dose and time dependent manner in HepG2 and Hep3B, whereas Pip showed no significant toxic effect. Synergistic effect of combined treatment with NaB, Cur and Pip on HCC cells was observed on cytotoxicity, apoptosis and cell cycle assay. Following in vitro studies, we performed RNA-seq transcriptome analysis on NaB, Cur and Pip and their combination on HepG2 and Hep3B cells. Transcriptome analysis reveals combined treatment of NaB, Cur and Pip induces anti-cancer activity in both of HCC cells.

HCC is a leading cause of cancer mortality worldwide[1]. Each year, approximately 800,000 new cases of primary liver cancer are reported, and a staggering 90% of these cases are attributed to HCC. The two-year survival rate in the US is less than 50%, and the five-year survival rate is only 10%[2,3]. HCC treatment line includes surgical resection, radiotherapy, chemotherapy and immunotherapy. Despite the achievements on the current treatment strategies, high recurrence rate and poor prognosis of HCC patients is still an issue[4]. Thus, new strategies are necessary for the diagnosis and treatment of HCC. Boron is a rare element showing biological functions in different organisms. Boron derivatives show therapeutic potential in different cancers such as hepatocellular carcinoma[5], multiple myeloma[6], breast[7] and small-cell lung cancer[8]. Bortezomib is the only boron containing chemotherapeutic drug approved for clinical use however, drug resistance rapidly develops in bortezomib treatment[9]. NaB is another boron derivative that is known to be an effective agent in obesity[10], wound healing[11], cryopreservation[12] and cancer[13]. NaB showed metabolic reprogramming related to SIRT3 activity in Hep3B cell lines[14].

Cur is the main hydrophobic polyphenol in the rhizome of the plant turmeric. Cur is known to have anti-inflammatory, antioxidant, anti-microbial and anti-cancer properties[15,16]. Cur induces apoptosis and autophagy in HCC. Despite curcumin's significant therapeutic value, the delivery of Cur is still an important issue as it shows photodegradation, short half-life, low bioavailability, and pharmacological activity[17]. Pip, isolated from black and long peppers, is an important plant alkaloid. It is known to improve curcumin's poor bioavailability by reducing the rate of its metabolic breakdown[18]. Combined treatment of Pip and Cur has been reported to

[1]Department of Genetics and Bioengineering, Faculty of Engineering, Yeditepe University, Kayısdagi Cad., Atasehir, 34755 Istanbul, Turkey. [2]Department of Molecular Biology and Genetics, Faculty of Natural Sciences, Istanbul University, 34134 Istanbul, Turkey. [3]Department of Molecular Biology and Genetics, Faculty of Engineering and Natural Sciences, Istanbul Sabahattin Zaim University, 34303 Istanbul, Turkey. [4]Molecular Biology and Genetics Department, Hamidiye Institute of Health Sciences, University of Health Sciences-Turkey, 34668 Istanbul, Turkey. [5]Experimental Medicine Research and Application Center, University of Health Sciences-Turkey, 34662 Istanbul, Turkey. ✉email: fsahin@yeditepe.edu.tr

enhance the anti-cancer effect in colorectal[19], leukemia[20] and breast[21] cancer cells. Furthermore, in vivo studies show that Cur and Pip combination treatment induced HCC in rats[22].

RNA-seq is a leading and high-throughput sequencing approach to provide insight into the transcriptome of a cell. Compared to previous Sanger sequencing- and microarray-based methods, RNA-Seq facilitates the discovery of novel transcripts, identification of alternatively spliced genes, and detection of allele-specific expression beyond quantifying gene expression[23]. Recent advances in the RNA-Seq workflow, from sample preparation to library construction to data analysis, have enabled researchers to further elucidate the functional complexity of the transcription. RNA-seq data analysis typically includes several steps: quality control, alignment, counting and normalization of the sequenced reads, and differential expression (DE) analysis[24,25].

In our study, RNA-seq transcriptome analysis was performed to examine the possible anti-cancer mechanisms of NaB, Cur and Pip combination exerting synergistic effect on HCC cells. First, cell viability of HepG2 and Hep3B cells were investigated under the treatment of NaB, Cur and Pip and their combination treatment. Next, apoptotic cell death and cell cycle analysis were determined for HepG2 and Hep3B cells treated with NaB alone or in combination Cur and Pip or in combination NaB, Cur and Pip (Fig. 1A). The in vitro studies were followed by RNA-seq transcriptome analysis to determine the synergistic effect on gene expression profiling and we verified the anti-cancer effect on functional and pathway analysis (Fig. 1B).

Results

Combination treatment of NaB, Cur and Pip inhibits growth of HCC cells.

To assess the drug interaction effect of NaB and Cur together, HepG2 and Hep3B cells were exposed to different concentrations of both drugs alone and in combination for 24, 48 and 72 h. NaB and Cur effectively inhibited growth of HepG2 cells in time and dose-dependent manner (Fig. 2A,B), while Pip treated cells showed no toxic effect except the highest dose (Fig. 2C). Combination treatment of NaB, Cur and Pip demonstrated significant cytotoxicity in time-dependent manner in HepG2 cells (Fig. 2D). Similarly, NaB and Cur effectively inhibited growth of Hep3B cells in time and dose-dependent manner (Fig. 3A,B). Pip treated cells showed no toxic effect (Fig. 3C) and combination treatment of NaB, Cur and Pip demonstrated significant cytotoxicity in time-dependent manner in Hep3B cells (Fig. 3D). HUVEC showed less toxicity compared to HCC cells when treated with a combination of NaB, Cur and Pip (Fig. S1).

The IC_{50} values of NaB and Cur against HepG2 cells for 48 h are 7664.5 µM and 44.8 µM, respectively. While the IC_{50} values of NaB and Cur against Hep3B cells are 6561 µM and 41.4 µM, respectively. Furthermore, combination of NaB and Cur was considered as a drug, as Pip improves the therapeutic effect and bioavailability of Cur. The CI value for NaB and Cur combination of 2.5 mM NaB and 30 µM Cur in HepG2 cells were calculated as 0.98. 1.7 mM NaB and 30 µM Cur combination treatment in Hep3B cells showed combination index (CI) value of 0.97. This demonstrated consistent synergy (CI < 1) between NaB and Cur, validate our selection criteria (Table S1).
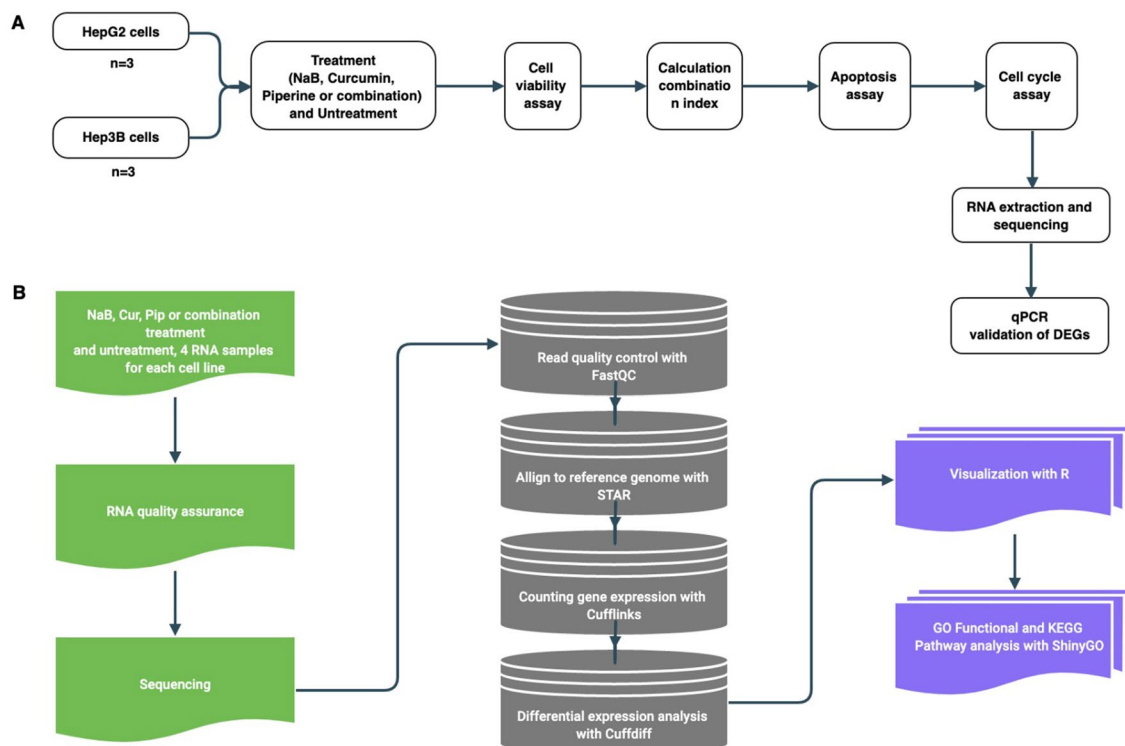

Figure 1. Study design: (**A**) Diagram representation of the experimental workflow. (**B**) The RNA-seq and bioinformatic analysis workflow.
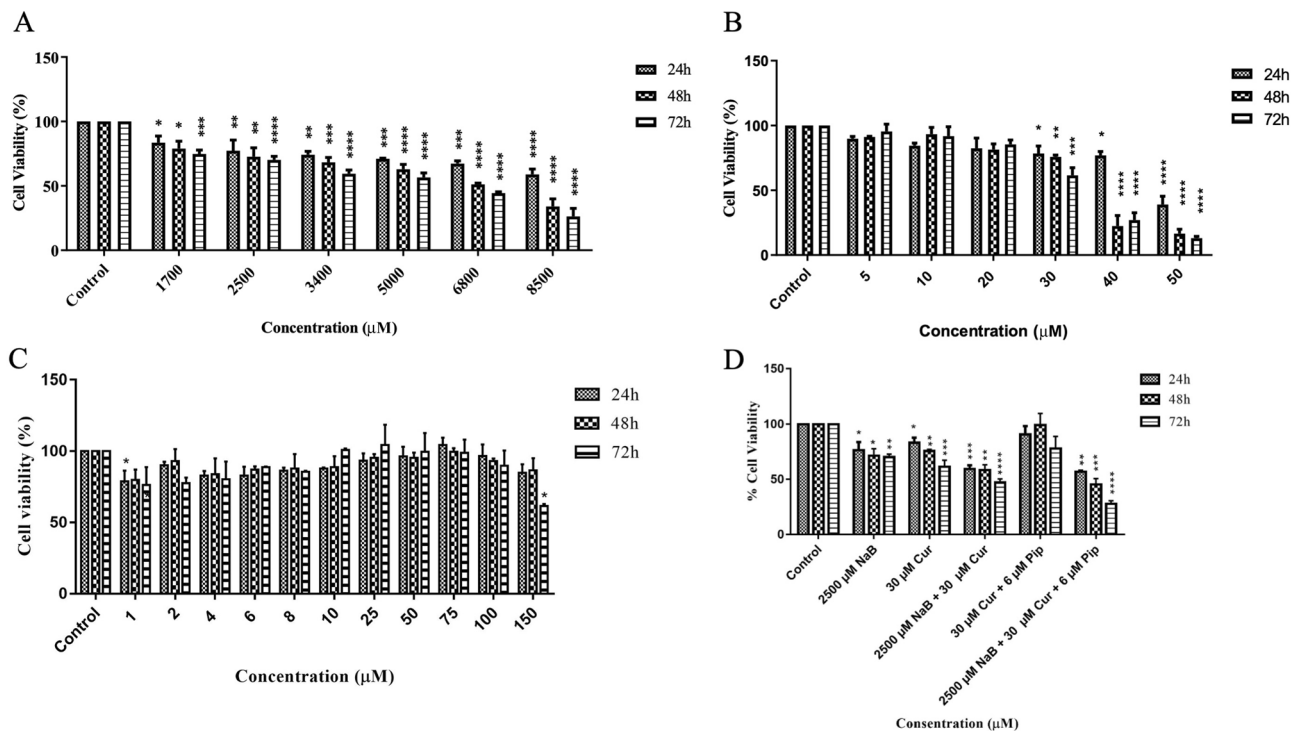
Figure 2. Effect of NaB, Cur, Pip and their combination treatment on cell viability of HepG2 cells. HepG2 Cells were incubated with (**A**) (1700–8500 μM) NaB, (**B**) (5–50) μM of Cur, (**C**) (1–150) μM of Pip and (**D**) combinations of NaB, Cur and Pip for 24 h, 48 h and 72 h. The cell viability was determined by MTS assay. Data represent the mean ± SD of independent experiments (n = 3) and statistical significance was assessed by one way ANOVA.
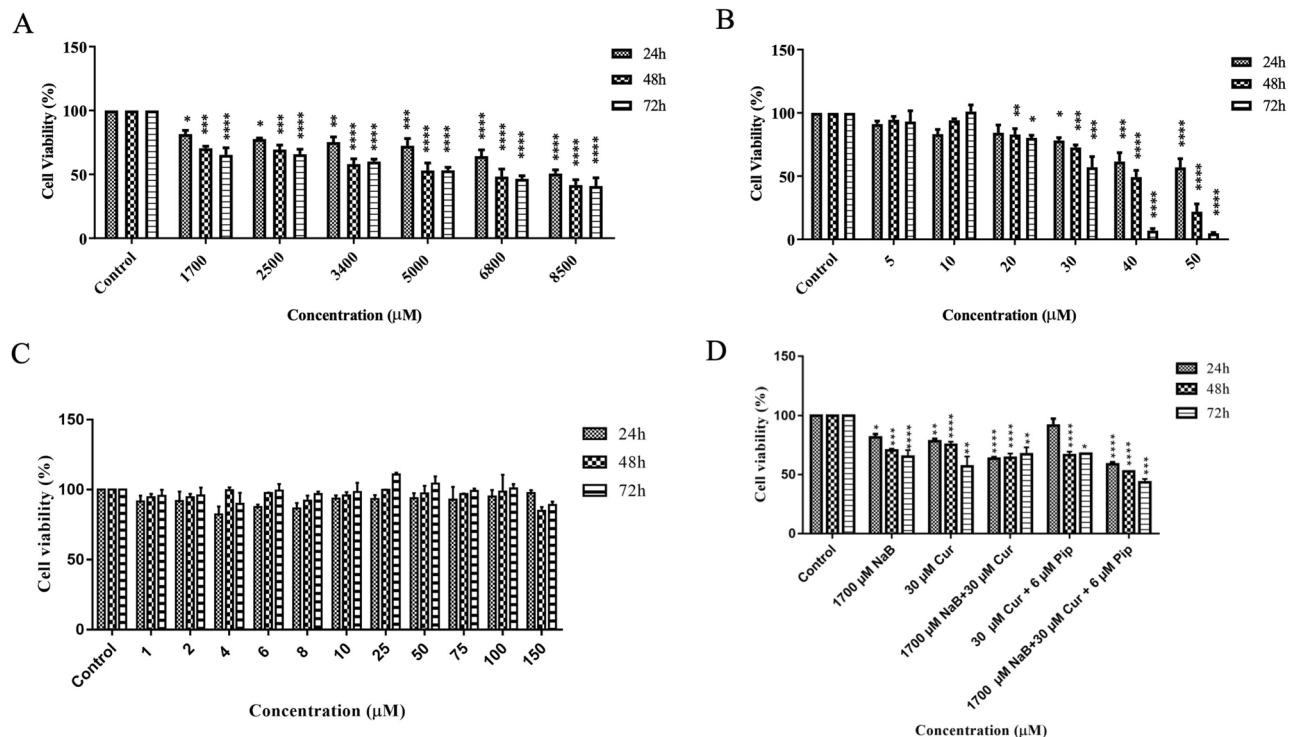

Figure 3. Effect of NaB, Cur, Pip and their combination treatment on cell viability of Hep3B cells. Hep3B Cells were incubated with (**A**) (1700–8500 μM) NaB, (**B**) (5–50) μM of Cur, (**C**) (1–150) μM of Pip and (**D**) combinations of NaB, Cur and Pip for 24 h, 48 h and 72 h. The cell viability was determined by MTS assay. Data represent the mean ± SD of independent experiments (n = 3) and statistical significance was assessed by one way ANOVA.

Combination treatment of NaB, Cur and Pip induce apoptosis and arrest the progression of cell cycle in HCC. Annexin V/PI apoptosis assay was performed to determine the apoptotic cell death percentage (representing the early and late apoptosis) after treating HCC cells with combination treatment of NaB, Cur and Pip. Autofluorescence for each cell line was established with an unstained control. Before each reading compensation procedure is performed for untreated samples using propidium iodide (PI) only, FITC only and FITC-PI double labelled standards. Our results showed that NaB, Cur and Pip combined treatment induced apoptosis in HepG2 and Hep3B cells, showing nearly 40% apoptotic cell death (Fig. 4A). To investigate the mechanisms underlying changes in cell cycle progression of HCC cells when treated with combination of NaB, Cur and Pip flow cytometry was used. As shown in Fig. 4B, our results suggest that combination of NaB, Cur and Pip inhibited cellular proliferation of HCC cell lines, HepG2 and Hep3B via arrested G0-G1 phase of the cell cycle.

RNA-seq transcriptome analysis of HCC under combination therapy of NaB, Cur and Pip. We performed RNA-seq transcriptome analysis on NaB, Cur and Pip and their combinations on HCC cells. The quality control of the sequencing read files with FastQC and the quality of the reads is shown in Fig. 5. We carried out the mapping of reads using STAR. The read and mapped number of HepG2 and Hep3B cells treated with NaB alone, Cur and Pip, combination of all three and untreated groups were shown in Fig. 6. The BAM output files were processed with Cufflinks for the detection of expression counts for downstream analysis. We evaluated the differentially expressed genes (DEGs) after FPKM normalization, and found total of 3143 genes ($P < 0.01$ and $\log_2 FC$(fold change) $> |1.5|$) at Cuffdiff, and at least 64 counts in any sample). In Fig. S2 was shown the dispersion plot and the scatter plot of distribution of all of the expressed genes in HepG2 and Hep3B data. We showed number of up-down regulated and Venn diagrams analysis of common genes after NaB, Cur, Pip or combination treatment ($P < 0.01$, $\log_2 FC$(fold change) $> |1.5|$) in Fig. 6.

The top 20 enriched Gene Ontology (GO) terms in the categories and KEGG pathway terms for DEGs in HepG2 and Hep3B after combination treatment were shown in Fig. 7A–D, respectively. The enriched functions of the DEGs in both of HCC cells include apoptotic process, regulation of biological quality and catalytic activity and related cell death terms. Also, the results and KEGG pathway enrichment analysis showed that the genes regulated by combination therapy were significantly involved in cancer-related pathways such as apoptosis, ferroptosis, cellular senescence, cell cycle, p53 signaling pathway, MAPK signaling pathway, IL-7 signaling pathway and TNF signaling pathway.

A heatmaps of the genes associated with the apoptotic process is shown in Fig. 8A and B. The gene expression patterns from untreated cells to NaB or Cur and Pip treatment were similar than that from untreated cells to combination treatment within the GO apoptosis process term. Furthermore, some similar synergistic effected genes to a provided expression profiles after combination treatment were shown in Fig. 8C.
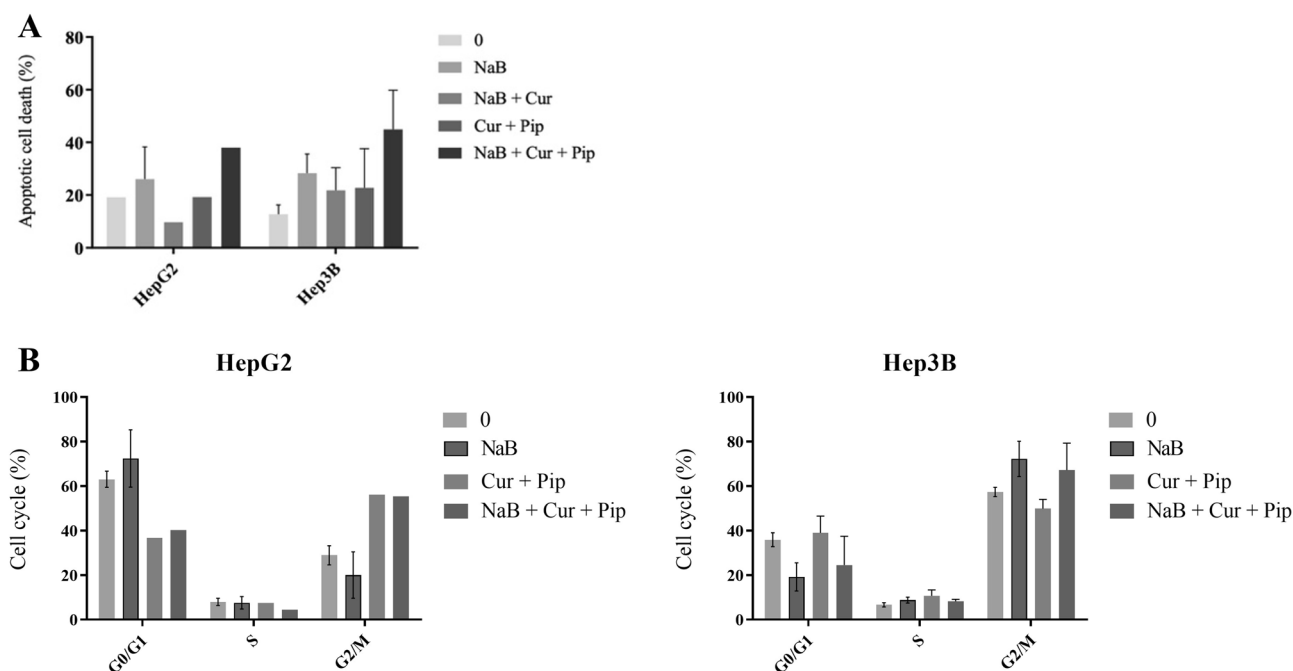

Figure 4. (**A**) The percentage of cells undergoing apoptotic cell death in HepG2 under 2500 µM NaB, 30 µM Cur and 6 µM Pip treatment, and Hep3B cells under 1700 µM NaB, treatment at 48 h. (**B**) Effect of NaB, Cur and Pip on cell cycle progression in HCC cell lines. Percentage of cell cycle profiles in HepG2 and Hep3B cells under NaB, Cur and Pip treatment at 48 h was analyzed by flow cytometry.
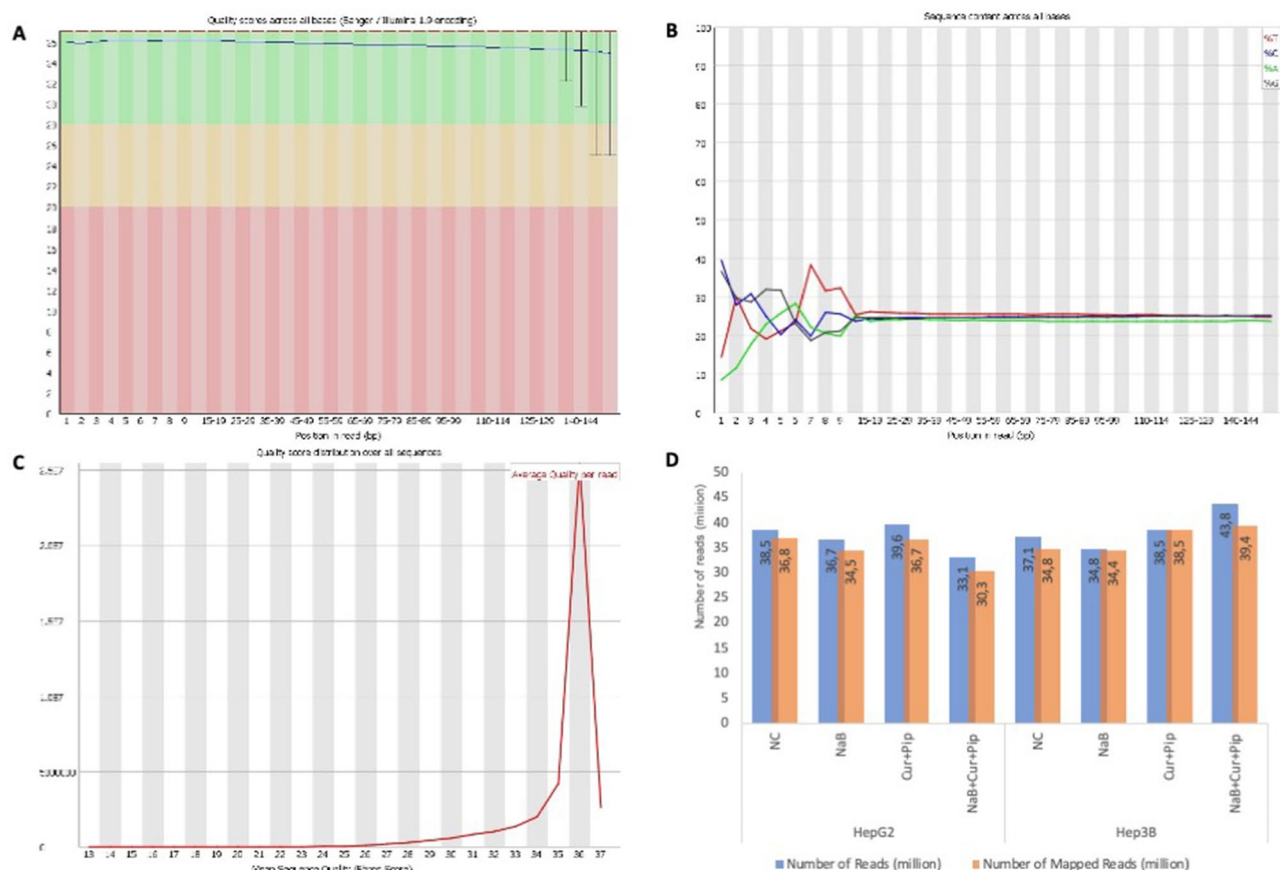
Figure 5. Quality control and statistics of the sequenced reads. (**A**) Distribution of quality scores by base pair. (**B**) The nucleotide content (A, T, C and G) in sequenced reads. (**C**) Distribution of the mean quality score by read. (**D**) The number of reads and mapped reads in HepG2 and Hep3B cells RNA-seq data.

Validation of the RNA-seq results using qRT-PCR. To validate the results of DEGs (p-value < 0.05) in transcriptome sequencing, *GADD45A* (Growth Arrest and DNA Damage Inducible Alpha), *BBC3* (BCL2 Binding Component 3) *CDKN1A* (Cyclin Dependent Kinase Inhibitor 1A), *PMAIP1* (Phorbol-12-Myristate-13-Acetate-Induced Protein 1) and *SERPINE1* (plasminogen activator inhibitor-1, PAI-1) which are apoptotic cell death related genes were selected for qRT-PCR. Compared to the NaB or Cur alone treated HepG2 cells, *GADD45A*, *BBC3*, *PMAIP1* and *SERPINE1* were up-regulated in combination treated groups (Fig. S3A). On the other hand, the combination treatment of NaB, Cur and Pip up-regulate *GADD45A*, *CDKN1A*, *PMAIP1* and *SERPINE1* genes in Hep3B cells compared to NaB or Cur alone treated groups (Fig. S3B).

Discussion

HCC is a common type of cancer that is caused by cirrhosis of the liver[26]. It is the most malignant primary human liver cancer, which is the sixth most common diagnosed cancer type and the third cause of cancer-related deaths in the world[27,28]. First line therapy methods include surgical, radiotherapy and chemotherapy[29]. However, poor therapeutic profile and high recurrence rate leads for the need of new strategy approaches and effective anti-cancer agents in treatment of HCC.

Various new agents besides chemotherapeutic drugs for cancer treatments have recently been discovered and boron-based agents are one of the forefront agents[27]. Studies have shown that boron derivatives have lethal effect on cancer cells by inhibiting cell division and increasing apoptosis. It can be used as anti-cancer agents in various cancers, such as the breast, lung, and prostate[30]. Previously, we have demonstrated that sodium perborate causes anti-proliferative and apoptotic effect in HepG2 and Hep3B cell lines[5]. NaB, also a boron derivative, is an effective agent cancer and shows SIRT3 activity in HCC Hep3B cell lines[14]. Although these boron derivative molecules show anti-cancer effect on HCC cells, high killing doses are needed. Thus, combination therapy is applied by combining two or more anti-cancer agents to increase the effectiveness of the agents on cancer cells and create a synergistic effect. It is also a treatment that can develop more effective cancer drugs[31].

Cur shows anti-proliferative, apoptotic, and anti-oxidative properties on many cancers, along with its pharmacological effects in many cancer types[32]. However, limitations on pharmacological activity of Cur along with its low bioavailability and short half-life[17], is a major issue to be used as anti-cancer agent alone. Studies show that Pip solves this problem by improving Cur's poor bioavailability[18] and enhances anti-cancer effect in many cancer cells[19,20]. Furthermore, Cur can be used alone or in combination with other drugs, targets signaling pathways
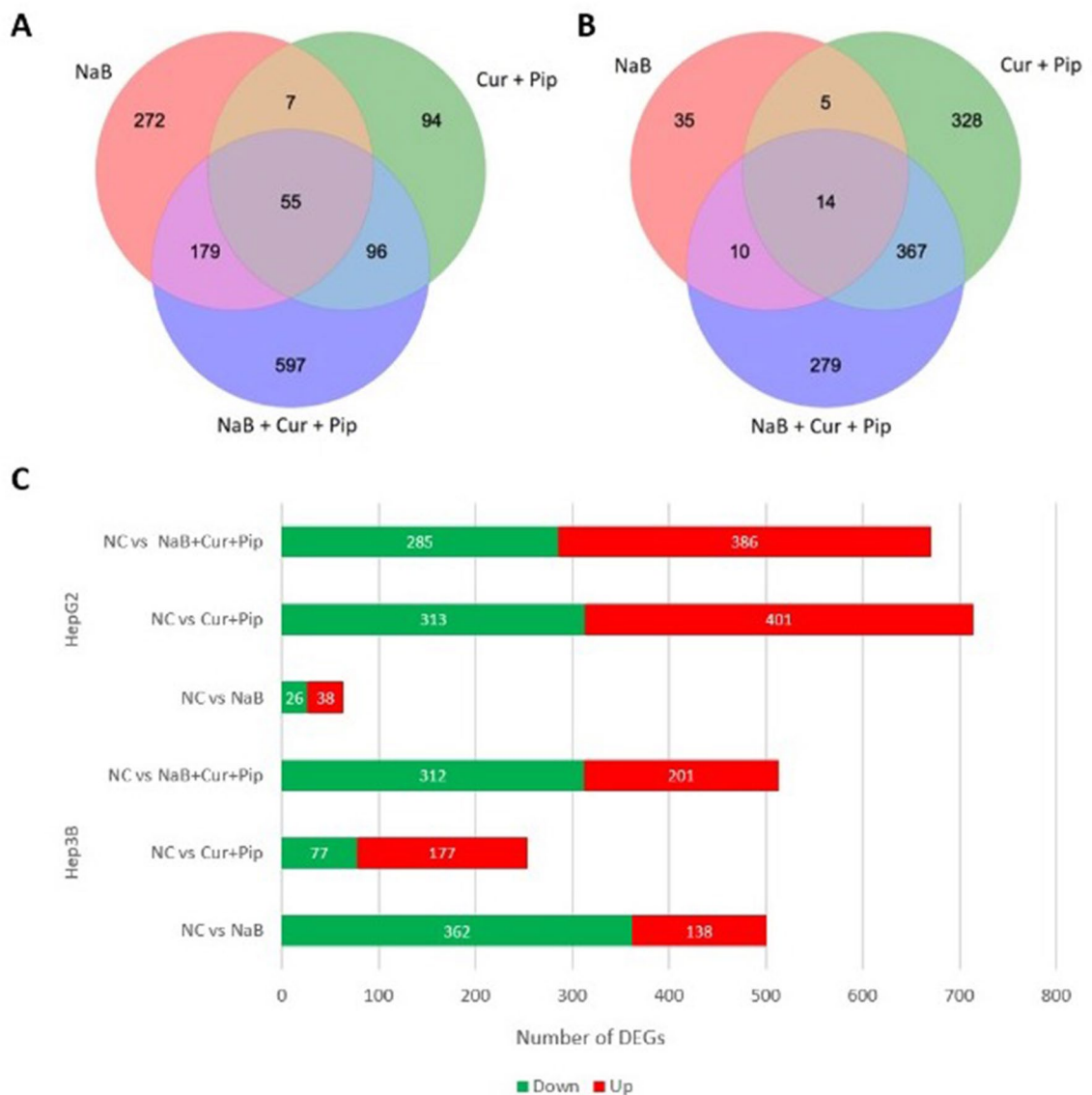
Figure 6. The overview of DEGs identified by RNA-seq analysis. (**A**) The Venn diagram shows NaB, Cur and Pip and their combination DEGs in HepG2 cells. (**B**) The Venn diagram shows NaB, Cur and Pip and their combination DEGs in Hep3B cells. (**C**) The number of DE up-regulated (red) and down-regulated (green) genes in HepG2 and Hep3B cells.

that trigger cancer development[33]. Anti-cancer studies show that Cur composes a synergistic effect with different anti-cancer drugs such as the PI3K inhibitor[34] and erlotinib[35]. Cur and 5-fluorouracil showed synergistic effect on HCC cells, leading to an increase in efficacy of 5-fluorouracil and decrease of concentration usage of 5-fluorouracil[36]. When drugs used in chemotherapy are applied as monotherapy on cancer cells, both high doses are applied, and their effects on cells are weak. For this reason, combination studies are essential in cancer studies.

In this study, we aimed to create a synergistic effect in HCC HepG2 and Hep3B cell lines by combination treatment of NaB, Cur and Pip. The current study investigated the cytotoxic, cell cycle arrest and apoptotic cell death effects of NaB, Cur and Pip in HCC cells, alone or in combination therapy. In addition, RNA-seq analyses were used to explore the molecular mechanism of NaB, Cur and Pip on HCC cells, followed by RT-qPCR to perform validation studies.

To characterize the cytotoxic effect of NaB, Cur and Pip, we first investigated the cell viability of HepG2 and Hep3B cells treated with either alone or in combination of NaB, Cur and Pip. Our cytotoxicity results show that HCC cells treated with NaB, Cur or Pip alone demonstrated a decrease in cell viability in time and dose dependent matter. Recent studies show IC_{50} concentration of HepG2 cells with boric acid and sodium perborate was determined as 24 mM and 1.13 mM[37]. Our results showed that NaB treated alone HepG2 and Hep3B cells had an IC_{50} value of 7.6 mM and 6.5 mM.

In combination therapy the effective dose was decreased to 2.5 mM and 1.7 mM for HepG2 and Hep3B cells, respectively. Thus, it was observed that low concentrations of NaB, Cur and Pip formed a synergistic effect, statistically significantly reduced the cell viability of HepG2 and Hep3B cells according to the time and dose
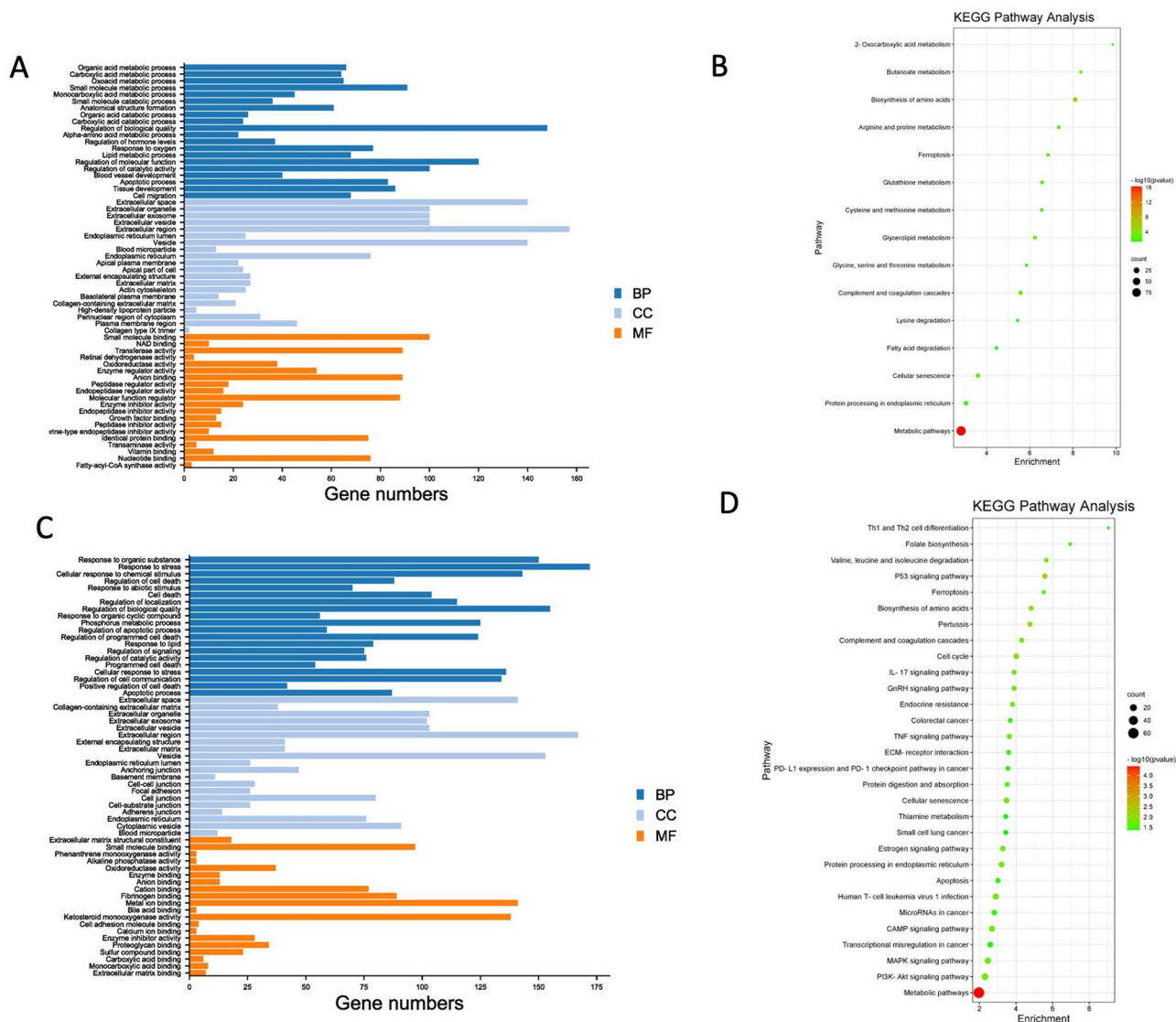
Figure 7. The top 20 Gene Ontology (GO) [Biological process (BP); Cellular component (CC), Molecular function (MF)] and KEGG pathway results for combination DEGs. (**A**) The GO results of combination DEGs in HepG2 cells. (**B**) The KEGG pathway results of combination DEGs in HepG2 cells. (**C**) The GO results of combination DEGs in Hep3B cells. (**D**) The KEGG pathway results of combination DEGs in Hep3B cells.

manner. When the CI value is CI < 1, it shows a synergy in combination treatment[38,39], thus our results show synergistic effect as the CI value for both HCC cells are less than one. Therefore, in this study we have shown that combination therapy NaB, Cur or Pip increased the effectiveness of the agents on cancer cells and create a synergistic effect by lowering the dosage of NaB.

To determine the effect of combination treatment of NaB, Cur and Pip on healthy cells, HUVEC was chosen as model cell line. Sodium perborate did not cause a significant decrease in cell viability of HUVEC cells compared to HCC cells[5] and our results are in consistency with literature as HUVEC showed less toxicity compared to HCC cells when treated with the same combination dosage of NaB, Cur and Pip.

Next, we investigated the apoptotic cell death and cell cycle progression in HCC cells when treated with NaB alone or combined with Cur and Pip. The combination study revealed that the apoptotic effect on cancer cells increased compared to alone treatment of NaB in HCC cells. Thus, combination treatment of NaB, Cur and Pip showed synergistic effect in apoptotic cell death of both HCC cells. Sodium perborate arrested cell cycle of HepG2 and Hep3B cells in G0/G1 phase[5]. Similarly, our results show that combination of NaB, Cur and Pip arrested HCC cells at G0-G1 phase.

To further explore the molecular mechanism of effect of NaB, Cur and Pip treatment and their combination treatment on two different HCC cells, we performed the gene expression profiling by RNA-seq on HCC cells. To identify genes regulated by NaB, Cur and Pip and their combination treatment, determine synergistic effect on gene regulation and further elucidate the molecular mechanism by which NaB, Cur and Pip combination inhibits HCC cell proliferation, transcriptome analysis were carried out on NaB, Cur and Pip, their combination treatment and non-treatment of HCC cells. A total of 671 and 513 DEGs were observed in NaB, Cur and Pip
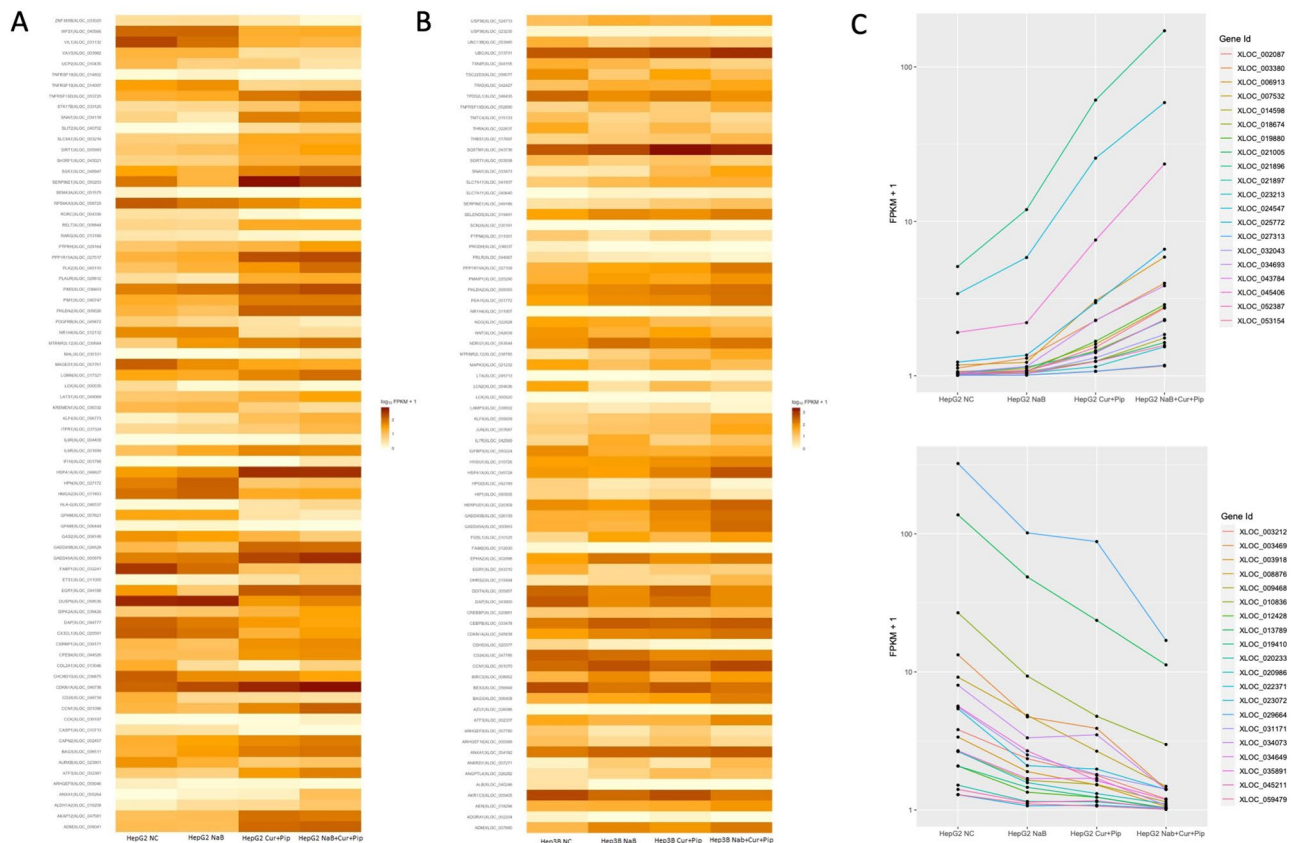
Figure 8. Heatmaps of combination DEGs in GO BP apoptotic process term and some similar effected combination DEGs. (**A**) The heatmap of DEGs after combination treatment in HepG2 cells. (**B**) The heatmap of DEGs after combination treatment in Hep3B cells. (**C**) The expression profiling of some synergistically affected DEGs in combination treatment.

combination treatment of HepG2 and Hep3B, respectively. These DEGs were further analyzed by GO functional enrichment which was annotated into biological process (BP), cellular component (CC), molecular function (MF) classifications and KEGG pathway enrichment analysis. The top 20 GO enriched classes and KEGG pathway results of combination DEGs of HepG2 and Hep3B cells are shown in Fig. 7. The GO results indicated that combination DEGs were significantly involved in apoptotic process GO term in both HCC cell lines and KEGG results showed that combination DEGs were significantly involved in cancer-related different signaling pathways such as apoptosis, ferroptosis, cellular senescence, cell cycle, p53 signaling pathway, MAPK signaling pathway, IL-7 signaling pathway and TNF signaling pathway. According to a previous study, the results of the microarray analysis of boric acid treated HepG2 cells showed that boric acid induced cell cycle, DNA replication and p53 signaling pathways[37]. Treatment of sodium perborate on HepG2 and Hep3B cells induced apoptosis and cell cycle related terms in RNA-seq GO and KEGG analysis[5], which is consistent with our results. Besides, an array-based study of Cur treated five HCC cell lines showed that up-regulated and down-regulated DEGs enriched in TNF signaling pathway, NF-kappa B signaling pathway, TGF-beta signaling pathway and AMPK signaling pathway[40]. Thus, our results were in consistent with literature (Fig. 7).

SERPINE1 plays an important role in p53 pathway[41] and PMAIP1 gene also inhibits proliferation and has a role in induction of apoptosis[42]. Previously we have shown that sodium perborate increases SERPINE1 and PMAIP1 genes expression in both HCC cells[5]. Similarly, our RNA-seq analysis of combination treatment of NaB, Cur and Pip in HepG2 and Hep3B cells showed increase in SERPINE1 and PMAIP1 genes expression. Furthermore, our results demonstrate an increase in GADD45A gene expression in HepG2 and Hep3B cells. GADD45A gene plays a essential roles in regulation of many cellular functions including DNA repair, cell cycle arrest control, pro-apoptotic activity and tumor growth suppression[43]. Besides, BBC3 gene shows a pro-apoptotic gene activity[44] and raises in HepG2 cells with treatment combination of NaB, Cur and Pip compared to NaB or Cur alone treated HepG2 cells. Also, in combination of NaB, Cur and Pip treated Hep3B cells, CDKN1A gene which has a role in regulation of cell cycle process[45] showed upregulated compared to NaB or Cur alone treated Hep3B cells. We have validated the accuracy of the RNA-seq data using RT-qPCR analyses.

In summary, our results demonstrated that combination treatment of NaB, Cur and Pip had synergistic effect in HepG2 and Hep3B cell lines. The combination of NaB, Cur and Pip inhibits cell proliferation and induces apoptosis in HCC cells compared to NaB or Cur alone treated HCC cells. We further examined the gene expression pattern of NaB, Cur and Pip treatment and their combination treatment on two different HCC cell lines using RNA-seq. According to these results, the expression level of some DEGs demonstrated the synergistic

effect in combination of NaB, Cur and Pip treated HCC cells compared to NaB or Cur alone treated HCC cells and NaB, Cur and Pip affected DEGs regulated several anti-cancer mechanisms. These findings suggested that combination of NaB, Cur and Pip may be a promising drug in the clinical treatment of HCC.

Materials and methods

Chemicals and reagents. NaB was purchased from National Boron Research Institute-BOREN (Ankara, Turkey). NaB stocks were prepared as 10 mg/mL in completed media using vortex and all solutions were filtered with a 0.22 μm filter before use. Cur and Pip were purchased from Sigma-Aldrich (St. Louis, MO, USA) and resuspended in dimethyl sulfoxide (DMSO) (Sigma-Aldrich, St Louis, MO) to prepare a stock solution of 50 mM and 150 mM, respectively. The main stock solution was filtered through a 0.22 μm filter and kept at − 20 °C for long time storage.

MTS reagent ([3-(4,5-dimethylthiazol-2-yl)-5- (3-carboxymethoxyphenyl)-2-(4-sulfophenyl)-2H-tetrazolium) was purchased from Promega (Southampton, UK). Annexin V-FITC Apoptosis Detection Kit was purchased from Roche (Germany). RNase A and PI were obtained from Sigma-Aldrich (Germany). Nonidet P-40 was obtained from AppliChem (Germany). RNeasy Mini kit, Sensiscript Reverse Transcription PCR Kit and QuantiTect SYBR Green PCR kit were supplied by Qiagen (United States).

Cell culture. Two different human HCC cell lines, HepG2 (HB-8065, ATCC), Hep3B (HB-8064, ATCC) were cultured in DMEM media supplemented with 10% fetal bovine serum (FBS) and 100 units/mL of penicillin, 100 μg/mL of streptomycin and amphotericin (1% PSA). HUVEC (CRL-1730) cell line, selected as normal cells, was maintained in DMEM media completed with 10% FBS and 1% PSA. All cells were incubated at 37 °C in a humidified atmosphere with 5% CO_2.

Cytotoxicity assay. The effect of NaB, Cur and Pip and their combination on both HCC and HUVEC cell lines were investigated using cell proliferation reagent MTS reagent assay. HepG2 (5×10^3 cells/well), Hep3B (5×10^3 cells/well) and HUVEC (5×10^3 cells/well) cells were seeded on 96 well plates. Cells were treated with (1700–8500) μM of NaB, (5–50) μM of Cur, (1–150) μM of Pip or combination of all three. At each 24 h interval, cells were incubated with appropriate MTS solution mixture for 2 h and absorbance was measured at 490 nm using a microplate spectrophotometer (Bio-tek ELx800, USA). Cell viability (%) was determined by setting non-treated control cells to 100%.

Combination index calculation. The multiple drug effect analysis of Chou and Talalay[38,39], which is based on the median-effect principle, was used to examine the nature of the interaction between NaB and Cur. Determination of the synergistic versus additive versus antagonistic cytotoxic effects of the combined treatment of cells with only NaB, only Cur and combination of NaB and Cur were assessed using the CI. The CI < 1, CI = 1 and CI > 1 indicate synergistic, additive and antagonistic effects, respectively. The CI was calculated using the following formula:

$$CI = [(D_1)/(D_x)_1] + [(D_2)/(D_x)_2]$$

where: $(D_x)_1$, $(D_x)_2$ = the concentrations of NaB and Cur that induced a 50% inhibition of cell proliferation; (D_1), (D_2) = the concentrations of NaB and Cur in combination that also inhibited cell growth by 50%.

Apoptosis and cell cycle assay. The relative percentage of apoptotic HepG2 and Hep3B cells and cell population percentages to NaB, Cur and Pip and their combination of all three were analyzed by Annexin V/PI assay kit (Roche, Cat. No. 11988549001) and cell cycle assay using flow cytometry. HepG2 cells were treated with 2500 μM NaB, 30 μM Cur and 6 μM Pip and their combinations, while Hep3B cells were treated with 1700 μM NaB, 30 μM Cur and 6 μM Pip and their combinations. For apoptotic cell death, pellets were collected after 48 h treatment, suspended in 1X annexin binding buffer and stained at room temperature for 15 min with 5 μL Annexin-V FITC and 5 μL PI according to manufacturer's protocol. Samples were analyzed immediately by Becton Dickinson FACS calibur flow cytometer with 20,000 events. For cell cycle arrest analysis, cells were trypsinized, washed by 1 × PBS and fixed in 70% ethanol solution for 1 h at − 20 °C. After fixation, cells were washed twice with ice cold 1 × PBS and stained with a cell cycle solution containing 10 μg/mL RNase A, 0.01% non-idet P-40 and 8 μg/mL PI for 30 min. Guava easyCyte Flow Cytometer (Merck Millipore, Germany) was used to determine cell population percentages of samples.

RNA preparation and sequencing. Total RNA was isolated from sampling for the HCC cell lines (HepG2 with 2500 μM NaB, 30 μM Cur + 6 μM Pip, 2500 μM NaB + 30 μM Cur + 6 μM Pip and without treatment for 48 h; Hep3B 1700 μM NaB, 30 μM Cur + 6 μM Pip, 1700 μM NaB + 30 μM Cur + 6 μM Pip and without treatment for 48 h) with RNeasy Mini RNA isolation kit (Qiagen; Valencia, CA, USA) in triplicate following the manufacturer's protocol. We measured RNA concentration using the Nanodrop 2000 Spectrophotometer (Thermo scientific). RNA quality was confirmed to be more than 8.0 RIN value. RNA-seq libraries were conducted with the NEBNext Ultra II Directional RNA Library Prep Kit (New England Biolab, Ipswich, Massachusetts, USA), according to the manufacturer's instructions. Finally, library quality was assessed on the Fragment Analyzer platform (Agilent Technologies, CA, USA). The resulting libraries were sequenced on the Illumina Novaseq 6000 System (Illumina, San Diego, USA) at Eurofins Genomics (Konstanz, Germany), resulting on approximately 30.3 to 43.8 million reads for each sample in a 2×150 bp pair-end.

RNA-seq data and downstream analysis. Quality control and reads statistics were determined by FastQC program[46]. The clean reads were then mapped to the human reference genome (GRCh38) using STAR alignment tool under default settings[47]. Following the mapping, the transcripts assembly of each sample was done with Cufflinks program[48]. Then the output GTF files were merged into a single unified transcript using the Cuffmerge program. The merged transcripts were compared to the reference annotation using the Cuffcompare program. The FPKM (the fragments per kilobase of transcript per million fragments) method was used to estimate the expression levels of mRNAs in every sample. Differential expression analysis in different treatment groups were performed using Cuffdiff software, an absolute value of |log2 (fold change)| > |1.5| and a p-value < 0.01 were set as the filter criteria for significant differential expression. These results were then interpreted using ShinyGO[49] for bioinformatics analysis to identify significant Gene Ontology (GO) functional terms BP, CC, MF and KEGG pathway[50] terms among the subsets of NaB, Cur and Pip and their combination treated and untreated groups.

Quantitative real-time-PCR (qRT-PCR) validation. RNA samples from NaB, Cur and Pip and their combination treated and untreated cells used for the RNA-seq were analyzed by qRT-PCR. First- strand cDNA was synthesized using Sensiscript Reverse Transcription PCR Kit qRT-PCR was performed on a CFX96 Real-Time PCR Detection System (Bio-Rad, Hercules, CA, USA) using QuantiTect SYBR Green PCR kit according to the manufacturer's protocol. Primers specific for *GADD45A* (forward, 5′-AGAAGACCGAAAGGATGGATA AGG-3′; reverse, 5′-CGGCCCGGGTTGCTGAC-3′), *CDKNA1* (forward, 5′-AGGGGACAGCAGAGGAAG -3′; reverse, 5′-GCGTTTGGAGTGGTAGAAATCTG-3′), *BBC3* (forward 5′-ACGACCTCAACGCGCAGT A-3′; reverse, 5′-CTAGTTGGGCTCCATTTCTGG-3′), *PMAIP1* (forward, 5'-AGATGCCTGGGAAGAAG-3′; reverse 5′-AGTCCCCTCATGCAAGT-3′), *SERPINE1* (forward, 5′-CTTCCACCCGTCTCTCTG-3′; reverse, 5′-CTACCAGGCACACAAAAGC-3′). The relation mRNA expression levels were normalized to *GAPDH* (forward, 5′-GGAGCGAGATCCCTCCAAAAT-3′; reverse, 5′-GGCTGTTGTCATACTTCTCATGG-3′) gene and calculated using the $2^{-\Delta\Delta Ct}$ method.

Statistical analysis. All data were analyzed statistically using one-way ANOVA or two-tailed Student's t-test. GraphPad Prism (version 8.0.1) Software was used to perform statistical analysis and plotting the graph. The error bars represent standard error of the mean from at least three independent experiments. The significant level was set at $*P \leq 0.05$, $**P \leq 0.01$, $***P \leq 0.001$, $****P \leq 0.0001$.

Data availability

The sequencing data have been deposited at NCBI with BioProject Accession Numbers PRJNA848267. The transcript abundance file for each sample has been submitted and archived to the NCBI Gene Expression Omnibus (GEO; http://www.ncbi.nlm.nih.gov/geo/) under sample Accession Number GSE207439.

References

1. Bray, F. *et al.* Global cancer statistics 2018: GLOBOCAN estimates of incidence and mortality worldwide for 36 cancers in 185 countries. *CA Cancer J. Clin.* https://doi.org/10.3322/caac.21492 (2018).
2. Sia, D., Villanueva, A., Friedman, S. L. & Llovet, J. M. Liver cancer cell of origin, molecular class, and effects on patient prognosis. *Gastroenterology* **152**, 745–761 (2017).
3. Alqahtani, A. *et al.* Hepatocellular carcinoma: Molecular mechanisms and targeted therapies. *Medicina* **55**, 1–22 (2019).
4. Janevska, D., Chaloska-Ivanova, V. & Janevski, V. Hepatocellular carcinoma: Risk factors, diagnosis and treatment. *Maced. J. Med. Sci.* https://doi.org/10.3889/oamjms.2015.111 (2015).
5. Omeroglu Ulu, Z., Bolat, Z. B. & Sahin, F. Integrated transcriptome and in vitro analysis revealed anti-proliferative effect of sodium perborate on hepatocellular carcinoma cells. *J. Trace Elem. Med Biol.* **73**, 127011 (2022).
6. Boccadoro, M., Morgan, G. & Cavenagh, J. Preclinical evaluation of the proteasome inhbitor bortezomib in cancer therapy. *Cancer Cell Int.* https://doi.org/10.1186/1475-2867-5-18 (2005).
7. Simsek, F. An in vitro study in which new boron derivatives maybe an option for breast cancer treatment. *Eurasian J. Med. Oncol.* https://doi.org/10.14744/ejmo.2018.0020 (2019).
8. Cebeci, E. & Fikrettin, S. Journal of trace elements in medicine and biology anti-cancer effect of boron derivatives on small-cell lung cancer. *J. Trace Elem. Med Biol.* **70**, 1–12 (2022).
9. Ling, X., Calinski, D., Chanan-Khan, A. A., Zhou, M. & Li, F. Cancer cell sensitivity to bortezomib is associated with survivin expression and p53 status but not cancer cell types. *J. Exp. Clin. Cancer Res.* **29**, 2–11 (2010).
10. Abdik, H. *et al.* Sodium pentaborate pentahydrate ameliorates lipid accumulation and pathological damage caused by high fat diet induced obesity in BALB/c mice. *J. Trace Elem. Med Biol.* https://doi.org/10.1016/j.jtemb.2021.126736 (2021).
11. Doğan, A. *et al.* Sodium pentaborate pentahydrate and pluronic containing hydrogel increases cutaneous wound healing in vitro and in vivo. *Biol. Trace Elem. Res.* https://doi.org/10.1007/s12011-014-0104-7 (2014).
12. Hayal, T. B. Boron increases the viability of human cancer and murine fibroblast cells after long time of cryopreservation. *Trakya Univ. J. Nat. Sci.* **2**, 115–122 (2020).
13. Aysan, E. *et al.* Effects of boron-based gel on radiation-induced dermatitis in breast cancer: A double-blind, placebo-controlled trial. *J. Investig. Surg.* https://doi.org/10.1080/08941939.2016.1232449 (2017).
14. Üstüner, B. & Çimen, H. Sodium borate treatment induces metabolic reprogramming in hepatocellular carcinoma through SIRT3 activation. *Turk. J. Biol.* **40**, 906–914 (2016).
15. Ghosh, S., Banerjee, S. & Sil, P. C. The beneficial role of curcumin on inflammation, diabetes and neurodegenerative disease: A recent update. *Food Chem. Toxicol.* https://doi.org/10.1016/j.fct.2015.05.022 (2015).
16. Shanmugam, M. K. *et al.* The multifaceted role of curcumin in cancer prevention and treatment. *Molecules* **1**, 2728–2769. https://doi.org/10.3390/molecules20022728 (2015).
17. Patil, V. M., Das, S. & Balasubramanian, K. Quantum chemical and docking insights into bioavailability enhancement of curcumin by piperine in pepper. *J. Phys. Chem. A* https://doi.org/10.1021/acs.jpca.6b01434 (2016).

18. Sehgal, A., Kumar, M., Jain, M. & Dhawan, D. K. Piperine as an adjuvant increases the efficacy of curcumin in mitigating benzo(a)pyrene toxicity. *Hum. Exp. Toxicol.* **31**, 473–482 (2012).
19. Bolat, Z. B. *et al.* Curcumin- and piperine-loaded emulsomes as combinational treatment approach enhance the anticancer activity of curcumin on HCT116 colorectal cancer model. *Front. Bioeng. Biotechnol.* **8**, 1–21 (2020).
20. Li, N., Wen, S., Chen, G. & Wang, S. Antiproliferative potential of piperine and curcumin in drug-resistant human leukemia cancer cells are mediated via autophagy and apoptosis induction, S-phase cell cycle arrest and inhibition of cell invasion and migration. *J. BUON.* **25**, 401–406 (2020).
21. Kakarala, M. *et al.* Targeting breast stem cells with the cancer preventive compounds curcumin and piperine. *Breast Cancer Res. Treat.* https://doi.org/10.1007/s10549-009-0612-x (2010).
22. Patial, V. *et al.* Synergistic effect of curcumin and piperine in suppression of DENA-induced hepatocellular carcinoma in rats. *Environ. Toxicol. Pharmacol.* https://doi.org/10.1016/j.etap.2015.07.012 (2015).
23. Finotello, F. & Di Camillo, B. Measuring differential gene expression with RNA-seq: Challenges and strategies for data analysis. *Brief. Funct. Genomics* https://doi.org/10.1093/bfgp/elu035 (2015).
24. Williams, C. R., Baccarella, A., Parrish, J. Z. & Kim, C. C. Trimming of sequence reads alters RNA-Seq gene expression estimates. *BMC Bioinform.* **103**, 1–13 (2016).
25. Choi, J. Guide: A desktop application for analysing gene expression data. *BMC Genomics* https://doi.org/10.1186/1471-2164-14-688 (2013).
26. Chidambaranathan-reghupaty, S., Fisher, P. B. & Sarkar, D. Hepatocellular carcinoma (HCC): Epidemiology, etiology and molecular classification. *Adv. Cancer Res.* **149**, 1–61 (2021).
27. Sperandio, R. C., Pestana, R. C., Miyamura, B. V. & Kaseb, A. O. Hepatocellular carcinoma immunotherapy. *Annu. Rev. Med.* **73**, 267–278 (2022).
28. Sugawara, Y. & Hibi, T. Surgical treatment of hepatocellular carcinoma. *Biosci. Trends* **15**, 138–141 (2021).
29. Zhong, C. *et al.* Clinical study of hepatectomy combined with Jianpi Huayu therapy for hepatocellular carcinoma. *Asian Pac. J. Cancer Prev.* **15**, 5951–5957 (2014).
30. Abdik, H. combined effects of zoledronic acid and sodium pentaborate pentahydrate on proliferation, migration and apoptosis of human neuroblastoma cell line. *Life Sci.* **7**, 24–35 (2021).
31. Guo, L., Li, H., Fan, T., Ma, Y. & Wang, L. Synergistic efficacy of curcumin and anti-programmed cell death-1 in hepatocellular carcinoma. *Life Sci.* **279**, 119359 (2021).
32. Ailioaie, L. M. Curcumin and photobiomodulation in chronic viral hepatitis and hepatocellular carcinoma. *Int. J. Mol. Sci.* **21**, 1–25 (2020).
33. Giordano, A. & Tommonaro, G. Curcumin and cancer. *Nutrients* **11**, 1–20 (2019).
34. Jia, T. *et al.* The differential susceptibilities of MCF-7 and MDA-MB-231 cells to the cytotoxic effects of curcumin are associated with the PI3K/Akt-SKP2-cip/kips pathway. *Cancer Cell Int.* **14**, 1–14 (2014).
35. Li, S. *et al.* Curcumin lowers erlotinib resistance in non-small cell lung carcinoma cells with mutated EGF receptor. *Oncol. Res.* **21**, 137–144 (2013).
36. Xu, T. *et al.* Synergistic effects of curcumin and 5-fluorouracil on the hepatocellular carcinoma in vivo and vitro through regulating the expression of COX-2 and NF-κB. *J. Cancer* **11**, 3955–3964 (2020).
37. Tombuloglu, A., Copoglu, H., Aydin-Son, Y. & Guray, N. T. In vitro effects of boric acid on human liver hepatoma cell line (HepG2) at the half-maximal inhibitory concentration. *J. Trace Elem. Med Biol.* **62**, 1–9 (2020).
38. Chou, T. C. Theoretical basis, experimental design, and computerized simulation of synergism and antagonism in drug combination studies. *Pharmacol. Rev.* https://doi.org/10.1124/pr.58.3.10 (2006).
39. Chou, T. C. & Talalay, P. Quantitative analysis of dose-effect relationships: The combined effects of multiple drugs or enzyme inhibitors. *Adv. Enzyme Regul.* https://doi.org/10.1016/0065-2571(84)90007-4 (1984).
40. Zeng, Y., Shen, Z., Gu, W. & Wu, M. Inhibition of hepatocellular carcinoma tumorigenesis by curcumin may be associated with CDKN1A and CTGF. *Gene* **651**, 183–193 (2018).
41. Wang, Z. *et al.* KIAA0101 up-regulates SERPINE-1 expression in p53 signalling pathway in gastric cancer. *Int. J. Clin. Exp. Med.* **12**, 11314–11323 (2019).
42. Do, H. *et al.* TFAP2C increases cell proliferation by downregulating GADD45B and PMAIP1 in non-small cell lung cancer cells. *Biol. Res.* **52**, 35 (2019).
43. Tamura, E. R. *et al.* GADD45 proteins: Central players in tumorigenesis. *Curr. Mol. Med.* **12**, 634–651 (2012).
44. Han, J. W. *et al.* Expression of bbc3, a pro-apoptotic BH3-only gene, is regulated by diverse cell death and survival signals. *Proc. Natl. Acad. Sci. USA* **98**, 11318–11323 (2001).
45. Di Giorgio, E., Gagliostro, E., Clocchiatti, A. & Brancolini, C. The Control operated by the cell cycle machinery on MEF2 stability contributes to the downregulation of CDKN1A and entry into S phase. *Mol. Cell. Biol.* **35**, 1633–1647 (2015).
46. Andrews, S. FastQC, Babraham Bioinforma. (2010)
47. Dobin, A. & Gingeras, T. R. Mapping RNA-seq reads with STAR. *Curr. Protoc. Bioinform.* https://doi.org/10.1002/0471250953.bi1114s51 (2015).
48. Trapnell, C. *et al.* Differential gene and transcript expression analysis of RNA-seq experiments with TopHat and Cufflinks. *Nat. Protoc.* https://doi.org/10.1038/nprot.2012.016 (2012).
49. Ge, S. X., Jung, D., Jung, D. & Yao, R. ShinyGO: A graphical gene-set enrichment tool for animals and plants. *Bioinformatics* **6**, 2628–2629 (2020).
50. Kanehisa, M., Furumichi, M., Sato, Y., Ishiguro-Watanabe, M. & Tanabe, M. KEGG: Integrating viruses and cellular organisms. *Nucleic Acids Res.* **49**, D545–D551 (2021).

Acknowledgements

Author contributions
Z.O.U., Z.B.B., N.S.D. and F.S. conceived the project and designed the experiments; Z.O.U., Z.B.B., N.S.D. performed the in vitro experiments and interpreted the results; Z.O.U. performed data analysis; Z.O.U., Z.B.B., N.S.D. wrote the paper; F.S. reviewed and edited the manuscript.

Competing interests
The authors declare no competing interest. A patent application with File Number 2022/005058 was recently accomplished to Turkish Patent and Trademark Office for the findings of this study.

Additional information

Supplementary Information The online version contains supplementary material available at https://doi.org/10.1038/s41598-023-40809-y.

Correspondence and requests for materials should be addressed to F.S.

Reprints and permissions information is available at www.nature.com/reprints.

Publisher's note Springer Nature remains neutral with regard to jurisdictional claims in published maps and institutional affiliations.